Published in : Journal of Raman Spectroscopy (2022), vol. 53, n°1, pp. 20–32
DOI: 10.1002/jrs.6249
Status : Postprint (Author's version)

APPLICATION OF THE ANALYTICAL QUALITY BY DESIGN PRINCIPLES TO THE DEVELOPMENT OF A QUALITATIVE SURFACE-ENHANCED RAMAN SCATTERING METHOD: A PROOF OF CONCEPT

Riccardo Deidda[1], Hermane T. Avohou[1], Elodie Dumont, Cédric Hubert, Philippe Hubert, Charlotte De Bleye[2], Eric Ziemons[2]

CIRM, Vibra-Santé HUB, Laboratory of Pharmaceutical Analytical Chemistry, University of Liège (ULiège), Liège, Belgium

[1]Riccardo Deidda and Hermane T. Avohou have equally contributed to this paper.

[2]Charlotte De Bleye and Eric Ziemons have equally contributed to this paper.

Keywords:

Analytical quality by design, AQbD, QbD, SERS, Surface-enhanced Raman scattering

Abstract

Analytical quality by design (AQbD) is a systematic approach that allows developing analytical methods in a more science-based way, due to the higher quality of information collected during the development process. However, its application remains limited to the development of separation methods. (i.e., liquid chromatography and capillary electrophoresis). Its application to spectroscopic techniques remains underexplored, despite the potential benefits. The aim of this work was to demonstrate the application of the AQbD principles to surface-enhanced Raman scattering (SERS) method development, detailing each step characterizing this approach. First, crystal violet (CV) was chosen as a model compound and the analytical target profile was defined. Risk assessment was performed to individuate the critical method parameters. The intensity of the CV band at 1175 cm^{-1} was selected as critical method attribute to be modeled and maximized. A screening study was conducted to study 11 aggregation agents (AAs) at different concentration levels (range 0.010–1 M) and in two solvent media (aqueous and methanolic). The two Aas exhibiting the strongest signal, one for each medium, were retained. Once these parameters were fixed, an I-optimal design was applied to optimize the entire analysis process. Here, the volumes of nanoparticle suspension and AA solution added to the SERS samples were simultaneously varied. Two method operable design regions, one for each medium, were computed using a Bayesian design space approach. The latter enabled evaluating the failure risk associated to each experimental condition explored and choosing those that best fit the analytical purpose in the experimental domain.

Published in : Journal of Raman Spectroscopy (2022), vol. 53, n°1, pp. 20–32
DOI: 10.1002/jrs.6249
Status : Postprint (Author's version)

1. INTRODUCTION

Surface-enhanced Raman scattering (SERS) is a Raman-based spectroscopic technique that is being increasingly used in analytical chemistry.[1–3] It consists in enhancing the Raman scattering by performing analyses with metallic surfaces such as silver or gold colloids, in the proximity of which analytes are adsorbed. That way the Raman effect can be drastically enhanced (by both electromagnetic and chemical mechanisms) and the low sensitivity of the conventional Raman scattering overcome.[4] Based on reported studies, an enhancement factor up to 10^3–10^6 can be achieved.[4,5] Consequently, molecules with high affinity for the metallic surface can be detected even at very low concentrations (from ppm to ppb). This makes the technique particularly interesting for qualitative methods such as analyte trace detection.[6]

Among the most used metals in SERS analysis, gold (AuNPs), silver, and copper nanoparticles are known to produce the highest signal enhancements.[1,7,8] SERS metal surfaces can be classified in three generic categories: metal nanoparticles (NPs) in suspension, metal NPs immobilized on solid substrates, and nanostructures fabricated directly on solid substrates.[9]

Specifically, NP suspensions can be obtained by chemical reduction, where a metal salt precursor (e.g., $HAuCl_4$ in the case of AuNP suspension) in solution is reduced by a reductant agent (e.g., sodium citrate).[10] This results in a simple and cheap procedure that does not require complex instrumentation and is easy to implement in a research laboratory.[7]

When using NP suspensions for SERS analysis, the use of an aggregation agent (AA) is recommended to enable the aggregation of NPs and consequently the formation of hot spots.[11] AAs have been the object of some work that focused on the understanding of their mechanism of action in complex matrices and their impact on Raman effect enhancement.[4,12–14] The main salts used as aggregation agents in SERS analysis are active electrolytes such as $AlCl_3$, KCl, NaCl, $ZnCl_2$, KBr, and NaF and passive electrolytes such as $ZnSO_4$, $MgSO_4$, and $NaNO_3$.[15] This classification is based on the ability of the salt ions to interact with SERS substrates. Indeed, active electrolytes can chemically interact with the colloidal substrate, displacing the stabilization agent and provoking changes in Zeta-potential, which leads to NP aggregation. Conversely, passive electrolytes do not interact with the substrate but cause NP aggregation by increasing the ionic concentration in the system.[16]

Concerning the applications of SERS in the pharmaceutical field, various SERS-based analytical methods are reported in the literature, as described by some recent reviews.[1–3] However, the implementation of this technique in quality control laboratories is still limited, despite its conveniences in terms of sensitivity. One of the major root causes of such situation is the lack of repeatability reported during quantitative analysis.[17]

Systematic approaches applied to SERS method development could be a sound and scientific way to promote SERS evolution and, as a consequence, its routine application. Such approaches enable gaining precious information about operational conditions of analytical methods and are increasingly applied in analytical chemistry. Indeed, pharmaceutical regulatory agencies are progressively encouraging the implementation of such approaches to cover the entire life cycle of pharmaceutical

Published in : Journal of Raman Spectroscopy (2022), vol. 53, n°1, pp. 20–32
DOI: 10.1002/jrs.6249
Status : Postprint (Author's version)

products, from manufacturing processes to quality control tests. In 2009, the International Council for Harmonization (ICH) of technical requirements for pharmaceuticals for human use proposed a systematic approach named "Quality by Design" (QbD) to be implemented in the pharmaceutical field.[18] In this context, the QbD strategy has also progressively been applied to analytical method development, since they are aimed to measure quality attributes (i.e., impurity profile and active pharmaceutical ingredient content) in pharmaceutical products.[19–23] The QbD applied to analytical chemistry is commonly named "Analytical Quality by Design" (AQbD).[22]

Nowadays, designs of experiments (DoE) are widely employed for modeling phenomena in analytical method development and optimization. It is a structured approach that allows correlating key responses to controllable variables.[24] For this reason, it is an integral part of the AQbD development process. In fact, a certain number of factors may potentially affect the critical method attributes (CMAs) of an analytical process in a negative or positive way. These factors are named critical method parameters (CMPs). In this context, the DoE strategy is employed as a chemometric tool to identify CMPs and then to deeply study how they affect CMAs.

However, the application of DoE by itself does not correspond to the application of the AQbD strategy. Indeed, the ICH Q8 guidelines define the concept of design space, the core of the QbD approach, as the "multidimensional combination and interaction of input variables and process parameters that have been demonstrated to provide assurance of quality."[18] Then, the concept of risk makes the difference in this context.[22] When it comes to analytical method development, the design space is named "method operable design region" (MODR). It consists of a multitude of possible working points, and for each of them, a specific probability of success (π) is given.[22,25,26] The concept of risk plays a central role in this strategy as the MODR is considered as a zone of theoretical robustness limited by the so-called edges of failure, outside of which the method performances are not accepted.[22]

In the last decade, the AQbD has been widely applied in both academia and pharmaceutical industries, mainly for the development of separation methods, involving different techniques such as liquid and supercritical fluid chromatography as well as capillary electrophoresis.[19,22] However, its implementation in the development of analytical methods based on spectroscopic techniques remains underexplored.[27]

The aim of the present work was to demonstrate the feasibility of applying the AQbD strategy also to the development of SERS methods. Indeed, in order to see major applications of SERS coming up in quality control laboratories in the future, more science-based approaches should be implemented and preferred when developing such methods.

In this study, a model compound, crystal violet (CV), was selected to develop an SERS qualitative method according to the AQbD principles. The whole development process focused on one of the characteristic bands of CV that was considered to measure the SERS enhancement for method optimization. To the best of our knowledge, this is the first application of the AQbD strategy to SERS method development documented in the literature. In fact, although DoE has already been applied in this context, the same cannot be said for the AQbD strategy.[7,28–30]

Published in : Journal of Raman Spectroscopy (2022), vol. 53, n°1, pp. 20–32
DOI: 10.1002/jrs.6249
Status : Postprint (Author's version)

2. MATERIALS AND METHODS

2.1 CHEMICALS AND REAGENTS

Gold (III) chloride hydrate (99.995% trace metals basis) was purchased from Sigma-Aldrich (St. Louis, MO, USA). Trisodium citrate (anhydrous, 98%) was purchased from Acros Organics (Geel, Belgium). Methanol (Ultra, HPLC-UHPLC grade) was purchased from J.T. Baker (Sowinskiego, Poland). Ultrapure water with a resistivity of 18.2 MΩcm was obtained from a Milli-Q device (Millipore, Bellirica, MA, USA). Crystal violet was purchased from TCI Europe N.V. (Zwijndrecht, Belgium), $AlCl_3$, KBr, Na_2HPO_4, NaCl, and $ZnCl_2$ from Merck (Darmstadt, Germany), and KCl, $MgSO_4$, NaF, $NaNO_3$, $ZnSO_4$, and $LiClO_4$ were purchased from VWR (Oud-Heverlee, Belgium).

2.2 SOLUTION PREPARATION

A stock solution of crystal violet was prepared in water at a concentration of 2×10^{-4} M. The stock solution was diluted to a concentration of 2×10^{-6} M in methanol (CV solution 1) and in water (CV solution 2).

A stock solution was prepared for each aggregation agent at the concentration of 1 M in water. This stock solution was diluted in water to the desired concentrations (1, 0.55, 0.5, 0.45, 0.4, 0.25, 0.1, 0.05, 0.01 M) during the study.

2.3 GOLD NANOPARTICLES

Gold nanoparticles were freshly synthesized by using the method described by Lee and Meisel.[10] Tetrachloroauric acid ($HAuCl_4$, 0.048 g) was dissolved in 100.0 ml of ultrapure water and heated to boiling point in a Drysyn heating block (Asynt, England). A solution of trisodium citrate 1% w/v (10.0 ml) was added using a dosing device (Dosimat, Metrohm AG, Switzerland) with a dropping rate of 5 ml min^{-1}. The resulting solution was kept boiling and under stirring for 1 h before being cooled down to room temperature.

The resulting NP suspension was then characterized by the means of different techniques before use.[7] Characterization results are displayed in **Table S1**. In order to avoid the effects due to a possible interbatch variability, the same NP suspension batch was used for the entire study.

2.4 EQUIPMENT

2.4.1 RAMAN SPECTROPHOTOMETER

All experiments were performed using a LabRAM HR Evolution Raman microscope (Horiba Jobin-Yvon, Lyon, France), equipped with a 785-nm laser (50 mW on the sample) and a two-dimensional EMCCD detector (1600 × 200 pixels sensor). Furthermore, the measurements were carried out with a 300 g/mm grating and the laser light was focused on the sample through a 50 × LWD objective (Leica, Wetzlar, Germany). The data were acquired in the 350–1750 cm^{-1} range. The confocal slit-hole, the exposition time, and number of repetitions were fixed at 200 µm, 3 s, and 3, respectively.

Published in : Journal of Raman Spectroscopy (2022), vol. 53, n°1, pp. 20–32
DOI: 10.1002/jrs.6249
Status : Postprint (Author's version)

2.4.2 AUNP CHARACTERIZATION

A Lambda 40 ultraviolet (UV)–visible spectrophotometer (Perkin Elmer, Waltham, MA, USA) was used to calculate the UV maximal absorption wavelength. Mean particle diameter and mean Z-potential were obtained by means of a dynamic and electrophoretic light scattering (DLS and ELS) system on a Zetasizer Nano ZS (Malvern Instruments, Malvern, UK) instrument.

2.5 SERS ANALYSES

2.5.1 SERS SAMPLE

During method development, each SERS sample consisted of 200 µl of analyte solution mixed with 200 µl of AuNP suspension, and 50 µl of aggregation agent solution. A 96 microwell plate was used as a support to perform SERS analysis, placing 400 µl of SERS sample and focusing with the objective on the liquid surface. Each SERS analysis was performed in triplicate preparing three independent SERS samples, in order to manage the variability intrinsically linked to the technique during statistical data treatment.

2.5.2 MODR DEFINITION STRATEGY

In order to define the MODRs, the CMA (SERS intensity of a specific CV band) was used to assess the quality of the SERS enhancement. Risk assessment using an Ishikawa diagram followed by screening DoE were used to identify the CMPs. Optimization designs and polynomial regression were then used to identify the best explanatory model of the relationships between the CMA and the CMPs.[31] This model was then used to assess the quality of the SERS enhancement in the whole multidimensional space defined by the CMPs. This is done by estimating a predictive probability distribution, which predicts future CMA values at each condition in that analytical space. This probability distribution is the key to the definition of the MODR, as it enables to assign to each condition of the experimental domain a probability of success or failure with respect to a specification, λ_0. It is the distribution of the CMA accounting for uncertainties related to both model parameters and intrinsic variations of the method. It can be derived by estimating the explanatory model using Bayesian multiple linear regression. The model was afterwards used to predict the SERS enhancement one can expect in the future at each condition, as proposed by Lebrun et al.[25] and Peterson and Lief.[32] This Bayesian approach is strongly recommended due to its recognized superior performance in risk management. The reader is referred to the textbook of Del Castillo for details on its rationale and technical implementation.[33]

This approach enables to define the MODR, which is the collection or set of any single point (i.e., combination of CMPs) denoted $\tilde{x}$ of the whole experimental domain denoted $\tilde{X}$ where the predicted CMA $\tilde{Y}$ meets its specifications λ_0 with a high probability say, at least π_0. Using a mathematical formalism, the MODR can be defined as (Equation 1):

$$\text{MODR} = \left\{\tilde{x} \in \tilde{X} : Prob\left(\tilde{Y} > \lambda_0 | \tilde{x}, \text{data}\right)\right] \geq \pi_0\}, \qquad (1)$$

where $\tilde{x}$ is any point (vector of CMPs) of the experimental domain $\tilde{X}$ whose CMA value is to be predicted, $\tilde{Y}$ is predicted value of the CMA at the analytical condition $\tilde{x}$, λ_0 is the acceptance limit for

Published in : Journal of Raman Spectroscopy (2022), vol. 53, n°1, pp. 20–32
DOI: 10.1002/jrs.6249
Status : Postprint (Author's version)

the selected CMA here taken to be 3000 a.u., π_0 is the quality level, that is, the minimum probability of acceptance, and $1 - \pi_0$ is the maximum risk of failure tolerated. The symbol "|" is read "given."

In the experimental part, two MODRs were calculated, one for each of the two solvents used for the analyte preparation namely methanol and water. The former was defined by the volume of AuNP suspension between 207 and 217 µl and the volume of AA solution between 43 and 33 µl. This volume range enables to achieve an SERS signal intensity equal or greater than λ_0 = 3000 a.u. with a minimum probability of π_0 = 75%. The latter was defined by the volume of AuNP suspension between 177 and 197 µl and the volume of AA solution between 73 and 53 µl. These volume ranges enable to achieve an SERS signal intensity equal or greater than λ_0 = 3000 a.u. with a minimum probability of π_0 = 95%.

2.6 SOFTWARE

The JMP® Pro 14 software (SAS Institute, Cary, North Carolina, USA) was used to generate all the experimental designs and to do preliminary analyses of the data.

Matlab R2018a (The Mathworks, Natick, MA, USA) and the PLS_Toolbox 8.6.2 (Eigenvector Research, Inc., Wenatchee, WA, USA) were used to preprocess Raman spectra and extrapolate SERS intensities. An automatic Whittaker filter (lambda = 100; p = 0.001) was applied as baseline correction tool. In addition, the Savitzky– Golay algorithm (derivative order, 0; window, 15; tails, polyinterp) was applied to smooth spectra.

A user-written R code was used to compute both Bayesian MODRs in RStudio® version 1.1.463 (RStudio Inc., Boston, MA, USA).[34]

3. RESULTS AND DISCUSSION

This section describes step by step the application of the AQbD strategy and consists of four parts: (i) analytical target profile definition, (ii) scouting phase, (iii) screening: critical method parameters, and (iv) Bayesian optimization and method operable design region definition. **Figure 1** depicts the AQbD workflow for method development.[22] As illustrated in this figure, the AQbD workflow has been interrupted after method development, because this work represents a proof of concept and a routine application was out of interest/scope. For this reason, the selection of a working point, its validation, and the routine application have been represented in light blue to underlight that they have not been carried out.

Published in : Journal of Raman Spectroscopy (2022), vol. 53, n°1, pp. 20–32
DOI: 10.1002/jrs.6249
Status : Postprint (Author's version)

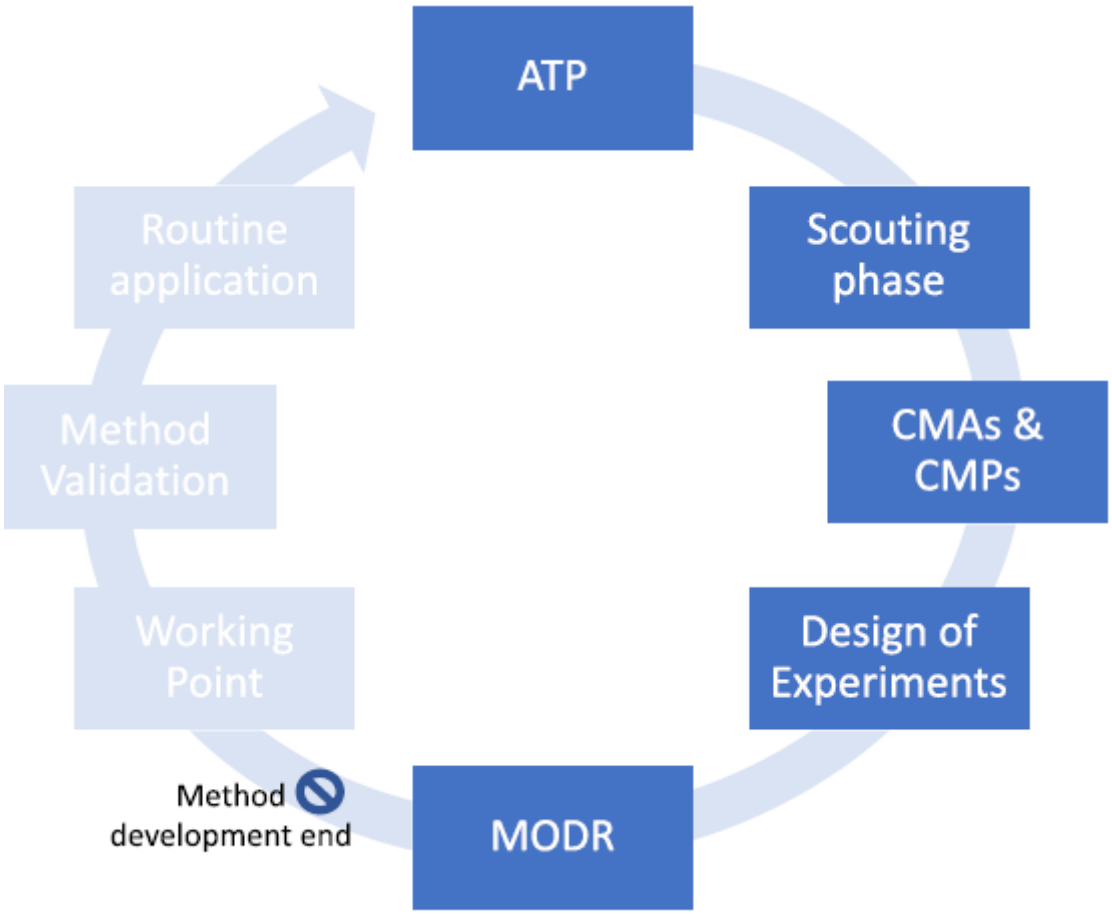

Figure 1. Analytical quality by design workflow

3.1 ANALYTICAL TARGET PROFILE DEFINITION

The first step of the AQbD strategy is the definition of the analytical target profile (ATP), which precisely defines what the method is supposed to measure. In this step, all the characteristics required for the method are accurately defined. In this case, the analytical target was crystal violet, which presents the following characteristic bands in its SERS spectrum: 805 cm^{-1} (out of plane ring C–H bend), 915 cm^{-1} (ring skeletal vibrations of radial orientation), 1175 cm^{-1} (in plane ring C–H bending), 1300 cm^{-1} (ring C–C stretching), and 1536, 1587, and 1620 cm^{-1} (ring C–C stretching).[35] The objective of the method was to define the optimal working conditions enabling the optimal detection (in terms of higher intensity of the 1175-cm^{-1} characteristic band) of CV with a defined probability of success. This intensity was measured as the highest point of the 1175-cm^{-1} band. CV was chosen as model compound because it gives an intense SERS response, due to the interaction between the nitrogen lone pair of its tertiary amino groups and the gold surface. Therefore, it is commonly used as a model compound to develop SERS methods or to conduct fundamental studies.[35–37] Another element that was taken into consideration was the solubility of CV in both water and alcohols, allowing the evaluation of the effect of the use of a different solvent as well. This aspect was essential for the study because the solvent present in the SERS medium affects the NP aggregation process and then the SERS enhancement.

Published in : Journal of Raman Spectroscopy (2022), vol. 53, n°1, pp. 20–32
DOI: 10.1002/jrs.6249
Status : Postprint (Author's version)

Furthermore, it is worth noting that in a pharmaceutical context, it is frequent to have media containing alcohols.

Figure 2 shows the complete SERS spectrum of CV (2×10^{-6}M) in aqueous (orange) and methanolic (blue) media and highlights the selected spectral band. The instrumental conditions used to obtain the spectra are described in Section 2.4.

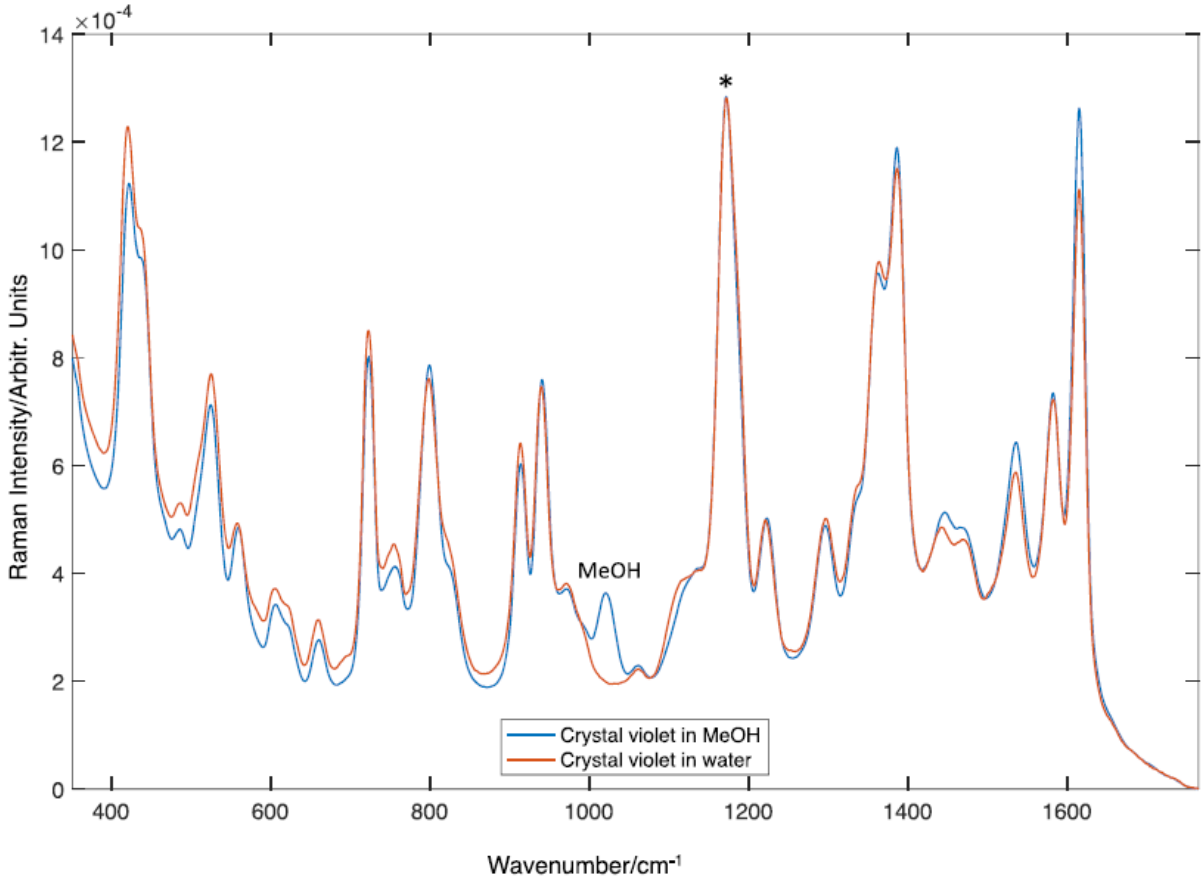

Figure 2. SERS spectra of crystal violet (2×10^{-6}M) with the selected band in aqueous (orange) and methanolic (blue) media. These spectra were acquired as follows: 250 µl of CV solution 2 was added to 250 µl of AuNPs suspension. As aggregation agent, 100 µl of solution of NaCl 0.1 M was used. The asterisk (*) highlights the CV band that was integrated in this study.

3.2 SCOUTING PHASE

Before planning the experimental study, preliminary experiments were necessary to investigate the analytical problem and set some parameters. These experiments also allowed properly defining the parameters and the experimental domain to investigate. In this context, different ways to prepare the SERS sample in terms of volumes of NP suspension, AA and analyte solutions, were explored using a univariate approach. Some experiments were also performed to evaluate the possibility to use methanol as the dilution solvent for the analyte and gain information about the effect of methanol on the SERS response and on the NP aggregation process. Methanol band was identified by comparing the spectrum of the CV dissolved in water (CV solution 2) with that of CV dissolved in methanol (CV solution 1), as clearly visible in **Figure 2**. Instrumental parameters were fixed as well based on prior knowledge.

Published in : Journal of Raman Spectroscopy (2022), vol. 53, n°1, pp. 20–32
DOI: 10.1002/jrs.6249
Status : Postprint (Author's version)

The scope of the SERS technique is to enhance the Raman effect to detect very low analyte concentrations that would otherwise be undetectable with conventional Raman spectroscopy. In this context, the parameters that can have an impact on this enhancement are of fundament importance and should be investigated to better exploit the potential of this analytical technique and satisfactorily fit the method purpose.

An Ishikawa diagram (**Figure S1**) was drawn to easily visualize and analyze all the parameters that potentially could impact the SERS analysis. This type of diagram, also called fish-bone diagram, is widely used in the AQbD context as a risk assessment tool. It is composed of various branches that represent different categories of risk related to the analytical technique. For SERS methods, these categories can be summarized in four groups of parameters: sample, instrument, SERS substrate, and SERS sample.[20,22,23] The parameters that were investigated as critical method parameters are colored in blue in **Figure S1**. These factors were prioritized and studied through design and analysis of experiments. This choice was made based on prior knowledge. Three successive screening factorial designs were used to study the aggregation agents and set their concentrations in the aqueous and methanolic media. Then, an I-optimal design was used to optimize the volume of AuNPs and define the method operable region using the Bayesian design space approach.

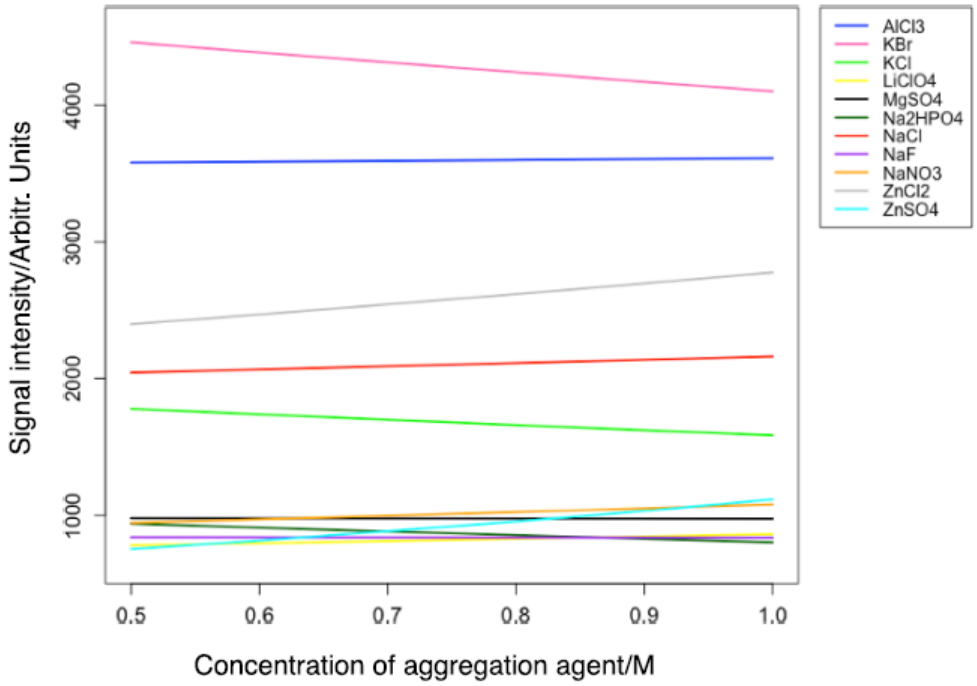

Figure 3. Regression plot for graphical representation of the results obtained from data treatment performed during the first screening study (CV in methanol)

3.3 SCREENING: CRITICAL METHOD PARAMETERS

Based on the results of the risk analysis, a first screening study using DoE was conducted. It focused on the selection of the best aggregation agent, because this process is critical to SERS analysis.[11] For this part of the study, CV was diluted in methanol at the concentration of 2×10^{-6}M (CV solution 1). Two factors related to the AA were then studied:

Published in : Journal of Raman Spectroscopy (2022), vol. 53, n°1, pp. 20–32
DOI: 10.1002/jrs.6249
Status : Postprint (Author's version)

a. The type of aggregation agent (AA type), a categorical factor with 11 different AAs, namely, $AlCl_3$, KBr, KCl, $LiClO_4$, $MgSO_4$, Na_2HPO_4, NaCl, NaF, $NaNO_3$, $ZnCl_2$, and $ZnSO_4$. These different AAs were selected to cover a large range of salts (including both active and passive electrolytes).
b. The concentration of AA (AA conc), a continuous factor at two levels (0.5 and 1 M). This high AA concentration range was first chosen to guarantee the efficiency of the NP aggregation process for each salt.

A two-factor full factorial design was used, implying the following model (Equation 2):

$$y = \beta_0 + X_1 + X_2 + (X_1 * X_2) + \varepsilon, \qquad (2)$$

where y is the selected band intensity, β_0 the intercept, X_1 the AA type, X_2 the AA concentration, and ε the error term.

Table 1. Analysis of variance table summarizing the effects of the type and concentration of aggregation agent (AA) on SERS intensity.

Factor	*df*	*F* value	*p* value	η^2
AA concentration	1	0.44	0.5065	0.001
AA type	10	156.11	0.0000	0.965
AA concentration: AA type	10	1.21	0.3056	0.007
Model	21	74.94	0.0000	0.973
Residuals	44	-	-	-

Note: R^2 adjusted, 0.9598.

The raw data are reported in **Table S2**, whereas the results of the statistical data treatment are presented in **Table 1**. The estimated model revealed that only the type of AA had a statistically significant effect on the CMA (**Table 1**, AA type: $p < 0.05$, **Figure 3**; see detailed statistical results in **Table S3**). Neither the AA concentration nor its interaction with the AA type were statistically significant (**Table 1**, AA conc: $p > 0.05$, AA type*AA conc: $p > 0.05$, **Figure 3**; see detailed results in **Table S3**), maybe due to the high AA concentration chosen. Five aggregation agents exhibited the highest intensities. These are all active electrolytes, namely, $AlCl_3$, KBr, $ZnCl_2$, NaCl, and KCl. This is likely due to their better ability to form hot spots on the metal surfaces. This is not surprising because, as mentioned above, active electrolytes can directly interact with the AuNPs causing the displacement of citrate ions from the NP surface and resulting, in certain conditions, in more effective signal enhancement. Citrate ions act as stabilization agents for NPs in suspension, avoiding their flocculation during storage. The migration of citrate ions from the NP surface causes an alteration of the Zeta-potential, provoking the NP aggregation. These five AAs were selected for further investigation at lower concentrations and in an additional solvent type used to dilute CV. It is worth noting that two of them achieved the highest intensities above 3000 a.u., namely, $AlCl_3$ and KBr.

Published in : Journal of Raman Spectroscopy (2022), vol. 53, n°1, pp. 20–32
DOI: 10.1002/jrs.6249
Status : Postprint (Author's version)

Based on the information gained from the first design, a second screening design was conducted first to better investigate the effect of lower AA concentrations on the SERS enhancement and second the effect of a new solvent (SV type), water. The lower concentrations were considered to investigate scenarios where insufficient amount of AA would cause inefficient aggregation of AuNPs in the medium. The latter was studied as new factor by selecting water and methanol as dilution solvents for the sample preparation step. This factor was introduced to obtain information about the impact of both solvents in the AuNP aggregation process.

Hence, the study included three AA concentrations, namely, 0.01, 0.05, and 0.1 M for each of the five previously selected AA, namely, $AlCl_3$, KBr, $ZnCl_2$, NaCl, and KCl.

A full factorial quadratic design was used, implying the following model (Equation 3):

$$y = \beta_0 + X_1 + X_1^2 + X_2 + (X_2 * X_1) + (X_2 * X_1^2) + X_3 + (X_3 * X_1) + (X_3 * X_1^2) + (X_2 * X_3) + (X_2 * X_3 * X_1) + \varepsilon, \quad (3)$$

where y is the selected band intensity, β_0 the model intercept, X_1 the concentration of AA, X_2 the type of AA, X_3 the type of solvent, and ε the error term.

This third model (Equation 3) enables to investigate how the linear or quadratic effect of AA concentration would change with either the aggregation agent or the solvent used, and how the linear effect of AA concentration would change with both AA type and SV type.

The raw data are reported in **Table S4**. The estimated model (Equation 3) showed that all interaction model terms were statistically significant (p values <0.05; **Table 2**) suggesting complex yet interesting interrelations between the AA, the solvent type, and the AA concentration as shown on **Figure 4** (see details of statistical results in **Table S5**). The effect of the type of AA on the intensity varied markedly with the solvent (**Figure 4**). For each solvent, the signal intensity was enhanced when increasing the concentration in this range, except for $ZnCl_2$ in methanol. This increase in the intensity was almost linear except the strong quadratic effect shown by NaCl and KCl in the methanolic medium. Over the whole concentration range, KBr exhibited the highest intensity in the methanolic medium, whereas $AlCl_3$ exhibited the highest intensity when performing the analysis in the aqueous medium.

To sum up, the dilution solvent played a key role on the SERS effect enhancement, as expected. Previous works have already pointed out the influence of this factor on NP aggregation, analyte solubilization, and occupation of active sites, and hence on SERS enhancement.[38–40] The AA concentration is also a crucial parameter that needs to be evaluated when developing SERS methods. This is obvious and more noticeable with NaCl and KCl, which showed a strong curvature with a maximum, that is, a phase of increasing intensity followed by a phase of decreasing intensity with the concentration (**Figure 4**). This phase of decrease might be due to an excessive aggregation, causing NP flocculation in the system.

Two AAs emerged from the previous screening study, enabling the highest intensities: KBr (for the methanolic medium) and $AlCl_3$ (for the aqueous medium). However, the maximum intensity recorded for each of them occurred at the edge of the experimental domain, suggesting optima might be found

Published in : Journal of Raman Spectroscopy (2022), vol. 53, n°1, pp. 20–32
DOI: 10.1002/jrs.6249
Status : Postprint (Author's version)

by extending the explored range. A third screening DoE was then set up, and hence, the same model as in Equation 3 was used to further investigate the presence of an optimal AA concentration within the working range of 0.25–0.55 M (0.25, 0.4, and 0.55 M). This is a full factorial quadratic design supported by the following model (Equation 4):

$$y = \beta_0 + X_1 + X_1^2 + X_2 + (X_2 * X_1) + (X_2 * X_1^2) + \varepsilon, \quad (4)$$

where y is the selected band intensity, β_0 the model intercept, X_1 the concentration of AA, X_2 the type of AA, and ε the error term.

Raw data are reported in **Table S6**. The estimation of the model (Equation 4) and optimization of the response surface showed an optimal concentration of 0.45 M for KBr, whereas for $AlCl_3$, the optimum was still at the edge of the domain, around 0.55 M (**Figure S3**; see detailed statistical results in **Tables S7** and **S8**).

To conclude, these results emphasize the importance of investigating the interactions between the type of AA and its concentration when developing an SERS method. These parameters are often fixed empirically or by trial and error, which do not enable to gain a sufficient understanding to efficiently set them. Even experiments using the one-factor-at-time approach can hardly lead to such a level of knowledge. The results also highlighted the importance of the influence of the solvent used in the SERS medium. An AA might enable strong enhancement with a solvent but a poor enhancement when another solvent is present in the analysis medium.

Table 2. Analysis of variance table summarizing the effects of the aggregation agent type (AA type), aggregation agent concentration (AA conc) and solvent type (SV type) on SERS intensity.

Factor	*df*	*F* value	*p* value
AA conc	1	82.01	0.0000
AA type	4	133.24	0.0000
SV type	1	76.13	0.0000
AA conc^2	1	18.40	0.0000
AA conc: AA type	4	29.28	0.0000
AA conc: SV type	1	18.30	0.0000
AA type: SV type	4	225.55	0.0000
AA type: AA conc^2	4	17.54	0.0000
SV type: AA con^2	1	9.49	0.0031
AA conc: AA type: SV type	4	10.10	0.0000
Model	25	89.43	0.0000
Residuals	60	-	-

Note: R^2 adjusted, 0.9613.

Published in : Journal of Raman Spectroscopy (2022), vol. 53, n°1, pp. 20–32
DOI: 10.1002/jrs.6249
Status : Postprint (Author's version)

3.4 BAYESIAN OPTIMIZATION AND DEFINITION OF THE METHOD OPERABLE DESIGN REGION

Once the best AA and its optimal concentration for each medium were defined, the study focused on the optimization of the quantity of each component, namely, the volume of AuNP suspension, AA and analyte solutions, to be mixed to constitute the SERS sample to analyze. During the previous phases indeed, these volumes were all kept constant at 200, 50, and 200 µl, respectively. The aim, at this stage, was to find an optimum proportion of AuNP suspension and AA solution enabling reaching the highest intensity for the 1175-cm^{-1} band. This targeted intensity was fixed to 3000 a.u. based on the knowledge and understanding gained from the previous screening designs. For that purpose, an I-optimal design including the volume of AuNP suspension as continuous factor was used. The volume of CV solution was still kept constant because the peak intensity is directly correlated to the concentration of analyte in SERS.

The model underlying the design was a fourth-degree polynomial model written as (Equation 5):

$$y = 1 + X_1 + X_1^2 + X_1^3 + X_1^4 + \varepsilon, \qquad (5)$$

where y is the CMA, X_1 is the volume of NP suspension added to the SERS sample, and ε is the error term.

This model was assumed because no sound prior knowledge about the relationship between this volume of AuNP suspension and the SERS intensity was available. Hence, a complex relation was assumed as a safe strategy with the hope that a more parsimonious model might be obtained through variable selection and model simplification during data analysis.

Figure S2 shows the SERS spectra obtained with each experimental condition while the model 5 was fitted to the data for each solvent using the Bayesian linear regression approach, described by Del Castillo.[33] Raw data are reported in **Table S9**. The posterior probability distribution of the parameters, accounting for uncertainties in their estimation, was derived. This enabled to obtain a Monte Carlo sample of size 6000 for each parameter of each model that represents its probability distribution. The means of estimated parameters are reported in **Table 3** as well as the Bayesian *p* values, which are interpreted here as the probability that the parameter is either greater or lower than 0. A model term is retained if its *p* value is greater than 0.95. The fourth-degree polynomial model was found relevant for $AlCl_3$ in aqueous medium (p values were greater than 0.95 for all model terms), whereas the three-degree polynomial was selected for KBr in methanolic medium as the quartic term was not relevant (*p* value <0.95). Using the selected models and the Monte Carlo sample of their parameters, the MODR was defined for each solvent by using the Bayesian design space approach as described in previous works[25,32,33] and summarized in Section 2.5.2. The so-called predictive distribution, accounting for both model error and model parameter uncertainties, is computed at 10,000 randomly sampled points or values of the volume of AuNPs in the experimental domain. For each sampled point of the domain, it is commutated by propagating the uncertainties from the Monte Carlo sample of the parameters to the selected model, enabling to have 6000 predicted values for any condition in the domain. It is interpreted as the distribution of the future intensity values of the SERS method at that condition. It was used to estimate the probability of being above the specification of 3000 a.u., at the corresponding

Published in : Journal of Raman Spectroscopy (2022), vol. 53, n°1, pp. 20–32
DOI: 10.1002/jrs.6249
Status : Postprint (Author's version)

condition. Computing that probability over the domain allowed generating the so-called "probability maps" or "risk-of-failure maps." These maps enabled to visualize the range of volumes meeting the specification with a high probability.

Table 3. Analysis of variance table for both SERS media

	$AlCl_3$ in aqueous medium			KBr in methanolic medium		
Model terms	**Mean**	***SE***	***p* value**	**Mean**	***SE***	***p* value**
Intercept	2895	0.87	1.000	2998	0.77	1.000
Volume	−4869	5.29	1.000	248.9	3.70	0.802
$Volume^2$	−2257	4.12	1.000	−594.1	5.10	0.977
$Volume^3$	3836	4.76	0.881	−528.5	4.90	0.957
$Volume^4$	5902	4.10	0.968	96.20	3.30	0.637

Note: *p* values: probability that the parameter is greater than 0.0 if its mean is positive or probability that the parameter is lower than 0.0 if its mean is negative; SE: standard error, $AlCl_3$: R^2 = 0.9114, adjusted R^2 = 0.9003; KBr: R^2: 0.2634, adjusted R^2: 0.1683.

In practical terms, the MODR was defined as the volume of AuNP suspension (and consequently the volume of AA solution added to prepare the SERS sample) that would enable to achieve with a high assurance an SERS signal intensity higher than the defined threshold (3000 a.u.). In this context, two MODRs were computed depending on the solvent used to dilute the analyte: one, named MeOH MODR, for analyses performed using methanol as the sample preparation solvent, and the other, named H_2O MODR, when water was used instead. **Figure 5** shows both MODRs. On this figure, the green area represents points (simulations) with intensities above the specification λ_0 = 3 000 a.u., whereas the red points are points that do not meet that specification. The vertical dotted lines delineate the MODR ranges, where the probability of success was observed to be the highest.

Specifically, the MODR in methanolic medium (MeOH MODR) was defined as the volume of AuNP suspension (horizontal axis, bottom) comprised between 207 and 217 µl and the volume of AA solution (horizontal axis, top) between 43 and 33 µl. These volume ranges enabled achieving an SERS signal intensity (vertical axis) greater than 3000 a.u. with a probability set at least 75%.

Concerning the aqueous medium, the MODR (named water MODR) was defined as the volume of AuNP suspension comprised between 177 and 197 µl and the volume of AA solution between 73 and 53 µl. These volume ranges enable to achieve an SERS signal intensity greater than 3000 a.u. with a probability of at least 95%.

It is interesting to notice that the MeOH MODR is narrower than the one computed for water. For the former, a lower minimum probability of success (75% against 95% for water) was achievable given the specification. A plausible explanation to these results could be a higher SERS signal variability occurring when performing analysis in the methanolic medium. In fact, because of its physical–chemical properties in terms of volatility, methanol is far from being an ideal solvent to perform SERS analysis.

Published in : Journal of Raman Spectroscopy (2022), vol. 53, n°1, pp. 20–32
DOI: 10.1002/jrs.6249
Status : Postprint (Author's version)

Another interesting phenomenon, which unveils on the probability maps is the fact that when working in the aqueous medium (**Figure 5**b), the set of experimental conditions allowing the satisfaction of the CMA specification is reduced in respect of that of the methanolic medium (**Figure 5**a). For the H_2O MODR, in the area going from 25 to 15 µl of AA solution volume, the probability of success is equal to zero, probably due to the aggregation inefficiency. In fact, in this area, NP aggregation does not occur at all and thus the Raman signal cannot be efficiently enhanced. This lack of aggregation was visually evident when performing the analyses. On the contrary, the methanolic medium seems to be less affected by the volume of AA added, resulting in a larger set of experimental conditions allowing obtaining SERS intensities higher than 3000 a.u.

These aspects underline one more time the importance of using systematic approaches when developing SERS methods in order to study and calculate the probability of success linked to experimental conditions that are employed by analytical methods.

The aim of this study was to showcase the AQbD application for method development and not to apply the method for routine use, as shown in **Figure 1**. Considering this latter eventuality, it is worth noting that, within the MODR, each point corresponds to a potential working point that can be selected as final experimental conditions. When opting for a working point, practical considerations should be done.[22] For instance, in this case, attention would be given to the error linked to the withdrawal of small quantities of liquids by automatic pipettes in a potential routine use. The highest volume of AA solution would be preferred. Furthermore, if the analytical target is soluble in both water and alcohols, as in this case, preference should be given to water, due to its ease of handling and higher probability of success of certain experimental conditions. After choosing a working point, validation studies have to be performed before applying the method to routine analyses.

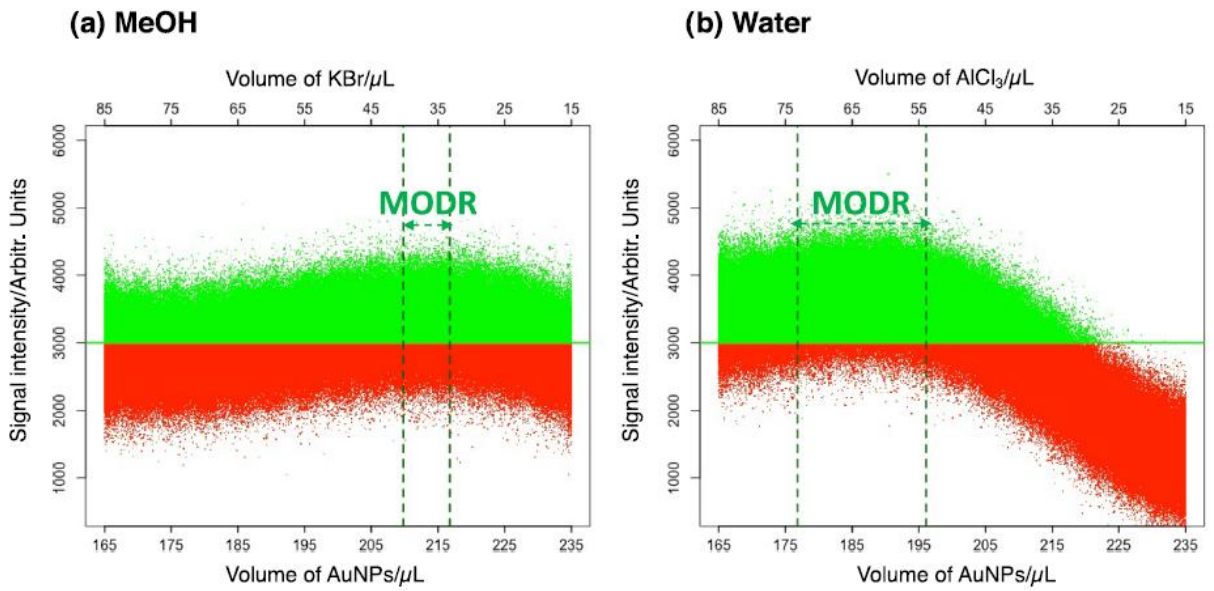

Figure 5. Method operable design regions for the analysis conducted in (a) MeOH and (b) water. The green area represents points with intensities above the specification λ_0 = 3000 a.u. while the red points are points which do not meet that specification. The vertical dotted lines delineate the MODR ranges

Published in : Journal of Raman Spectroscopy (2022), vol. 53, n°1, pp. 20–32
DOI: 10.1002/jrs.6249
Status : Postprint (Author's version)

4. CONCLUSIONS

The AQbD strategy is a convenient approach that allows obtaining relevant information about analytical methods under development. This is particularly interesting for methods that are potentially aiming at routine activity uses in a pharmaceutical context, but not only. Risk was evaluated at the very beginning of the method development process, allowing a proper risk management as recommended by ICH Q8.

In fact, precious information about the critical parameters influencing SERS analysis has been collected. The acquired knowledge allowed to properly fix these parameters to adequately fit the analytical purpose and manage the risk correlated to them.

Often, these parameters are set on the basis of insufficient preliminary experiences or a priori considerations without a pertinent exploration of other possibilities that could result in better solutions. The AQbD strategy can be very useful to analytical chemists in order to make more conscious choices when developing SERS methods, allowing to justify these choices, for instance to regulatory agencies when asking for marketing authorizations. In fact, the adoption of a more science-based approach in SERS method development could help to recognize the value of this analytical technique and to implement its use for measuring critical quality attributes of drug substances and products in quality control laboratories.

ACKNOWLEDGEMENT

The National Fund for Scientific Research, F.R.S. – FNRS is acknowledged for the Aspirant funding granted to E. DUMONT (1.A030.17 – FC6921).

CONFLICT OF INTEREST

The authors declare no conflict of interest.

AUTHOR CONTRIBUTION

Riccardo Deidda: writing (original draft), writing (review and editing), conceptualization, formal analysis, visualization; **Hermane T. Avohou**: writing (original draft), writing (review and editing), conceptualization, software; **Elodie Dumont**: writing (review and editing); **Cédric Hubert**: writing (review and editing); **Philippe Hubert**: supervision, funding acquisition, conceptualization, project administration; **Charlotte De Bleye**: writing (review and editing), conceptualization, supervision; **Eric Ziemons**: writing (review and editing), conceptualization, supervision, funding acquisition, project administration.

Published in : Journal of Raman Spectroscopy (2022), vol. 53, n°1, pp. 20–32
DOI: 10.1002/jrs.6249
Status : Postprint (Author's version)

DATA AVAILABILITY STATEMENT

The data that supports the findings of this study are available in the supplementary material of this article

SUPPLEMENTARY MATERIAL

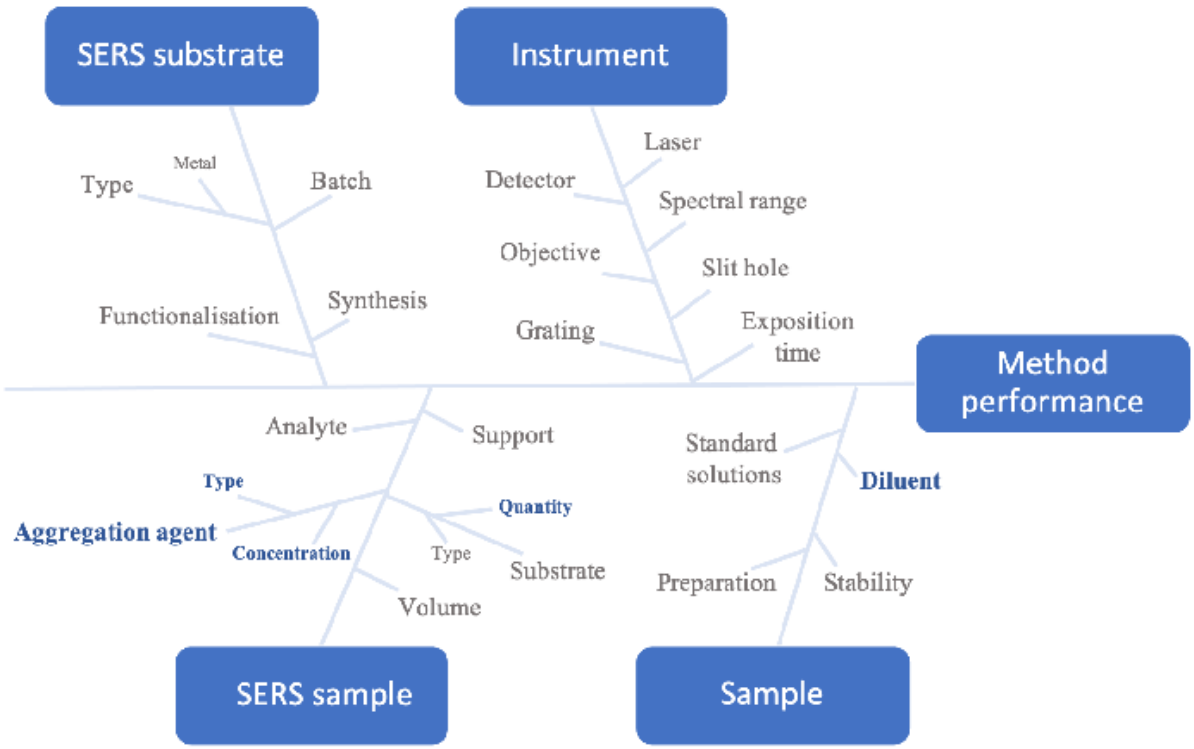

Figure S1. Ishikawa diagram for SERS methods.

Table S1. Results obtained from SERS substrates characterization.

Type	UV λ_{max} (nm)	*Mean particle diameter (n=3)(nm)*	*Mean Z-potential (n=3)(mV)*	*pH*	*Ionic strength ($\mu S\ cm^{-1}$)*
AuNPs	540.6	57.66	-45.63	5.37	841

AuNPs, gold nanoparticles; *UV* λ_{max}, UV maximal absorption wavelength.

Published in : Journal of Raman Spectroscopy (2022), vol. 53, n°1, pp. 20–32
DOI: 10.1002/jrs.6249
Status : Postprint (Author's version)

Table S2. Full factorial design for the first screening study (CV in methanol).

Exp. no.	*AA type*	*AA conc. (M)*	*Mean SERS intensity (n=3)(a.u.)*
1	$AlCl_3$	1	3610.85
2	KBr	1	4140.87
3	KCl	1	1590.37
4	$LiClO_4$	1	862.65
5	Na_2HPO_4	1	803.89
6	NaCl	1	2178.89
7	NaF	1	839.12
8	$NaNO_3$	1	1094.04
9	$ZnCl_2$	1	2779.20
10	$ZnSO_4$	1	1126.18
11	$MgSO_4$	1	974.72
12	$AlCl_3$	0.5	3604.87
13	KBr	0.5	4460.51
14	KCl	0.5	1786.45
15	$LiClO_4$	0.5	782.42
16	Na_2HPO_4	0.5	950.10
17	NaCl	0.5	2057.48
18	NaF	0.5	840.92
19	$NaNO_3$	0.5	948.39
20	$ZnCl_2$	0.5	2398.27
21	$ZnSO_4$	0.5	756.69
22	$MgSO_4$	0.5	979.05

Published in : Journal of Raman Spectroscopy (2022), vol. 53, n°1, pp. 20–32
DOI: 10.1002/jrs.6249
Status : Postprint (Author's version)

Table S3. Results, in terms of estimates, standard error and p-value from the statistical data treatment for the first screening study. The values in bold indicate the statistical significance.

Predictors	*Estimates*	*Std. Error*	*p value*
Intercept	1798.45	29.56	**<0.001**
AA conc	19.80	29.56	0.119
AA type 1	1809.41	93.48	**<0.001**
AA type 2	2502.24	93.48	**<0.001**
AA type 3	-110.04	93.48	**0.011**
AA type 4	-975.91	93.48	**<0.001**
AA type 5	-821.56	93.48	**0.017**
AA type 6	-921.46	93.48	0.104
AA type 7	319.73	93.48	**0.019**
AA type 8	-958.43	93.48	**0.001**
AA type 9	-777.24	93.48	**<0.001**
AA type 10	790.28	93.48	**0.005**
AA conc * AA type 1	-16.81	93.48	0.689
AA conc * AA type 2	-179.62	93.48	0.160
AA conc * AA type 3	-117.84	93.48	0.075
AA conc * AA type 4	20.31	93.48	0.518
AA conc * AA type 5	-21.97	93.48	0.585
AA conc * AA type 6	-92.90	93.48	**0.025**
AA conc * AA type 7	40.91	93.48	0.896
AA conc * AA type 8	-20.70	93.48	0.589
AA conc * AA type 9	53.02	93.48	0.294
AA conc * AA type 10	170.66	93.48	0.257
Observations, 66; R^2, 0.977; R^2 adjusted, 0.9598.			

Published in : Journal of Raman Spectroscopy (2022), vol. 53, n°1, pp. 20–32
DOI: 10.1002/jrs.6249
Status : Postprint (Author's version)

Table S4. Full factorial design for the second screening study.

Exp. no.	*AA type*	*AA conc. (M)*	*SV type*
1	NaCl	0.100	MeOH
2	$ZnCl_2$	0.010	MeOH
3	$AlCl_3$	0.100	H_20
4	KBr	0.055	MeOH
5	$AlCl_3$	0.055	H_20
6	$ZnCl_2$	0.055	MeOH
7	KCl	0.010	MeOH
8	$AlCl_3$	0.010	MeOH
9	KBr	0.010	H_20
10	$ZnCl_2$	0.010	H_20
11	NaCl	0.055	H_20
12	NaCl	0.010	H_20
13	NaCl	0.010	MeOH
14	$AlCl_3$	0.055	MeOH
15	$AlCl_3$	0.010	H_20
16	KBr	0.100	H_20
17	KCl	0.100	H_20
18	KBr	0.010	MeOH
19	KBr	0.100	MeOH
20	$ZnCl_2$	0.100	H_20
21	KCl	0.055	H_20
22	KCl	0.055	MeOH
23	$ZnCl_2$	0.055	H_20
24	KBr	0.055	H_20
25	$ZnCl_2$	0.100	MeOH
26	NaCl	0.100	H_20
27	$AlCl_3$	0.100	MeOH
28	KCl	0.010	H_20
29	NaCl	0.055	MeOH
30	KCl	0.100	MeOH

Exp. no, experiment number; *AA type*, type of aggregation agent; *AA conc.*, concentration of aggregation agent; *SV type*, solvent type.

Published in : Journal of Raman Spectroscopy (2022), vol. 53, n°1, pp. 20–32
DOI: 10.1002/jrs.6249
Status : Postprint (Author's version)

Table S5.

A) Results, in terms of estimates, standard error and p-value from the statistical data treatment for the second screening study in the aqueous medium. The values in bold indicate the statistical significance.

Predictors	*Estimates*	*Std. Error*	*p-value*
Intercept	841.48	31.35	**<0.001**
AA conc	8212.08	1476.58	**<0.001**
AA type 1	676.69	62.70	**<0.001**
AA type 2	-261.32	62.70	**<0.001**
AA type 3	-309.79	62.70	**<0.001**
AA type 4	-572.90	62.70	**<0.001**
(AA conc)^2	-17308.51	13064.05	0.195
AA conc * AA type 1	-7562.31	2953.17	**0.016**
AA conc * AA type 2	-9529.60	2953.17	**0.003**
AA conc * AA type 3	5887.65	2953.17	0.055
AA conc * AA type 4	22589.71	2953.17	**<0.001**
AA type 1 * (AA conc)^2	37382.02	26128.09	0.163
AA type 2 * (AA conc)^2	106211.39	26128.09	**<0.001**
AA type 3 * (AA conc)^2	-45729.74	26128.09	0.090
AA type 4 * (AA conc)^2	-180179.41	26128.09	**<0.001**

Observations, 45; R^2, 0.969 ; R^2 adjusted, 0.955.

B) Results, in terms of estimates, standard error and p-value from the statistical data treatment for the second screening study in the methanolic medium. The values in bold indicate the statistical significance.

Predictors	*Estimates*	*Std. Error*	*p-value*
Intercept	6279.92	64.59	**<0.001**
AA conc	59798.82	3042.22	**<0.001**
AA type 1	1630.45	129.18	**<0.001**
AA type 2	2546.48	129.18	**<0.001**
AA type 3	-2900.68	129.18	**<0.001**
AA type 4	-3469.54	129.18	**<0.001**
(AA conc)^2	-366021.08	26915.98	**<0.001**
AA conc * AA type 1	-50143.94	6084.44	**<0.001**
AA conc * AA type 2	-52415.14	6084.44	**<0.001**
AA conc * AA type 3	77216.95	6084.44	**<0.001**
AA conc * AA type 4	94131.00	6084.44	**<0.001**
AA type 1 * (AA conc)^2	333401.80	53831.96	**<0.001**
AA type 2 * (AA conc)^2	331313.01	53831.96	**<0.001**
AA type 3 * (AA conc)^2	-495654.21	53831.96	**<0.001**
AA type 4 * (AA conc)^2	-615134.24	53831.96	**<0.001**

Observations, 45; R^2, 0.990 ; R^2 adjusted, 0.986.

Published in : Journal of Raman Spectroscopy (2022), vol. 53, n°1, pp. 20–32
DOI: 10.1002/jrs.6249
Status : Postprint (Author's version)

Table S6. Custom design for the optimization study.

Exp. no.	*AA type*	*AA conc. (M)*	*SV type*	*Mean SERS intensity (n=3) (a.u.)*
1	$AlCl_3$	0.40	H_20	3636.07
2	$AlCl_3$	0.40	H_20	3629.33
3	KBr	0.25	MeOH	3193.29
4	KBr	0.40	MeOH	3230.89
5	$AlCl_3$	0.40	MeOH	3135.22
6	KBr	0.25	H_20	1941.31
7	$AlCl_3$	0.25	MeOH	2308.72
8	KBr	0.55	H_20	2166.22
9	KBr	0.40	MeOH	3332.25
10	$AlCl_3$	0.40	MeOH	3133.38
11	$AlCl_3$	0.55	MeOH	2741.35
12	$AlCl_3$	0.55	H_20	4590.60
13	KBr	0.40	H_20	2162.15
14	KBr	0.55	MeOH	3178.85
15	KBr	0.40	H_20	2216.31
16	$AlCl_3$	0.25	H_20	3013.65

Exp. no, experiment number; *AA type*, type of aggregation agent; *AA conc.*, concentration of aggregation agent; *SV type*, solvent type.

Table S7. Results, in terms of estimates, standard error and p-value from the statistical data treatment for the optimization study. The values in bold indicate the statistical significance.

Predictors	*Estimates*	*Std. Error*	*p-value*
Intercept	24049.82	1203.99	**<0.001**
AA conc	9044.47	6264.85	0.156
AA type 1	-663.30	1203.99	0.585
$(AA\ conc)^2$	-9218.42	7763.13	0.242
AA conc * AA type 1	3812.40	6264.85	0.546
AA type 1 * $(AA\ conc)^2$	-3305.69	7763.13	0.672

Observations, 48; R^2, 0.313; R^2 adjusted, 0.232.

Published in : Journal of Raman Spectroscopy (2022), vol. 53, n°1, pp. 20–32
DOI: 10.1002/jrs.6249
Status : Postprint (Author's version)

Table S8. Analysis of variance table of the effects of the AA conc and AA type on SERS intensity.

Factor	*Df*	*Sum Sq*	*Mean Sq*	*F-value*	*Round*
AA conc	1	1505536.2	1505536.2	4.11	0.0490
AA type	1	4193056.1	4193056.1	11.45	0.0016
$(AA\ conc)^2$	1	516248.81	516248.81	1.41	0.2417
AA conc*AA type	1	736482.73	736482.73	2.01	0.1635
AA type: $(AA\ conc)^2$	1	66385.15	66385.15	0.18	0.6724
Residuals	42	15376932.2	366117.43	-	-

R^2, 0.3134; R^2 adjusted, 0.2316.

Table S9.

A) Custom design for the optimization of SERS analysis conditions in water.

Exp. no.	*AuNP volume (µL)*	*AA volume (µL)*	*Mean SERS intensity (a.u.)(n=3)*
1	180	70	3621.26
2	200	50	3491.98
3	223	27	1909.08
4	200	50	3422.09
5	165	85	3575.08
6	180	70	3453.51
7	200	50	3578.20
8	223	27	1765.08
9	235	15	1262.07
10	180	70	3702.60

Exp. no, experiment number; *AuNP volume*, volume of gold nanoparticle suspension; *AA volume*, volume of aggregation agent solution.

Published in : Journal of Raman Spectroscopy (2022), vol. 53, n°1, pp. 20–32
DOI: 10.1002/jrs.6249
Status : Postprint (Author's version)

B) Custom design for the optimization of SERS analysis conditions in MeOH.

Exp. no.	*AuNP volume (µL)*	*AA solution volume (µL)*	*Mean SERS intensity (a.u.)(n=3)*
1	180	70	2997.38
2	200	50	3266.12
3	223	27	3446.65
4	200	50	3302.13
5	165	85	2872.57
6	180	70	2907.47
7	200	50	3387.96
8	223	27	3116.07
9	235	15	3030.46
10	180	70	2823.66

Exp. no, number of experiment; *AuNP volume*, volume of gold nanoparticle suspension; *AA volume*, volume of aggregation agent solution.

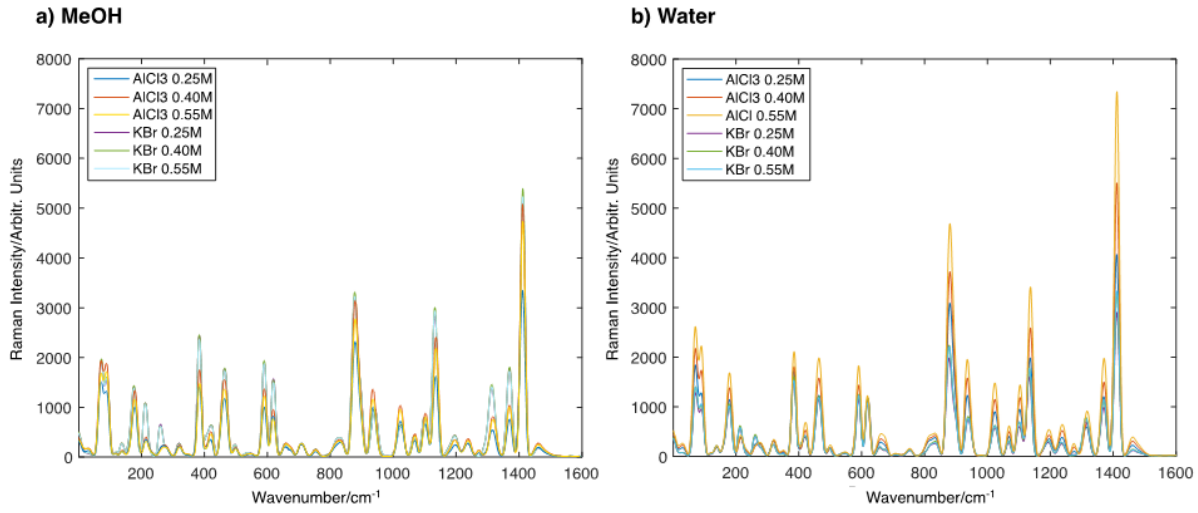

Figure S2. SERS spectra obtained during the optimization study.

Published in : Journal of Raman Spectroscopy (2022), vol. 53, n°1, pp. 20–32
DOI: 10.1002/jrs.6249
Status : Postprint (Author's version)

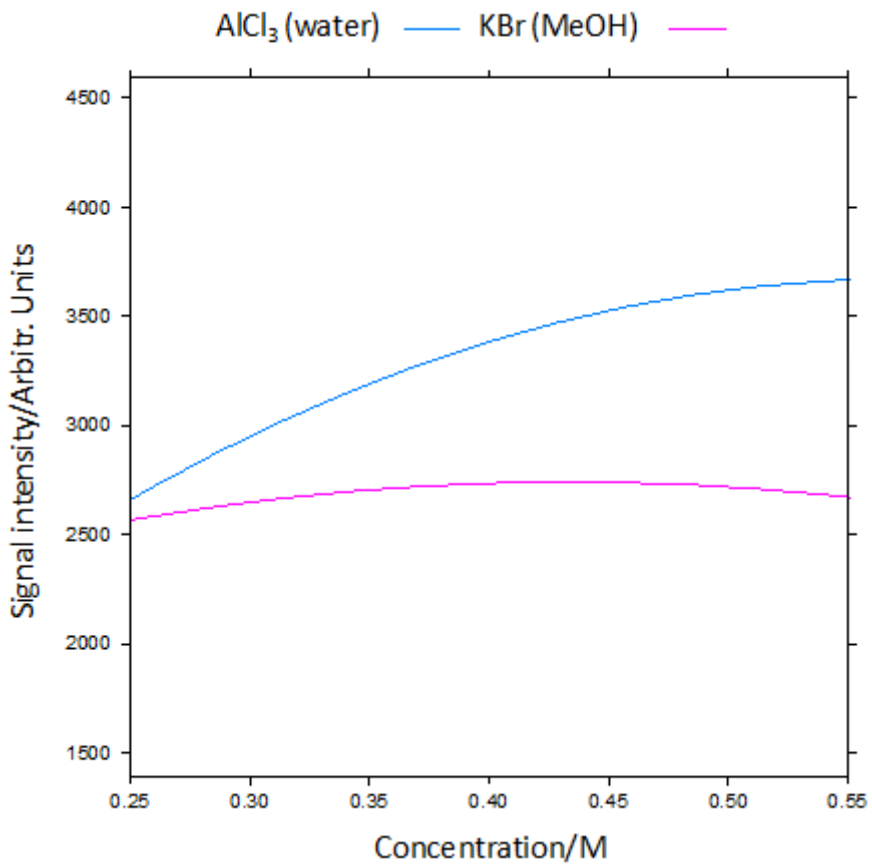

Figure S3. Effect of concentration on the signal intensity for the two AAs during the last phase of the screening study about AAs.

ORCID

Riccardo Deidda: https://orcid.org/0000-0002-8548-8038
Elodie Dumont: https://orcid.org/0000-0003-4798-1937

REFERENCES

[1] J. Cailletaud, C. De Bleye, E. Dumont, P.-Y. Sacré, L. Netchacovitch, Y. Gut, M. Boiret, Y.-M. Ginot, P. Hubert, E. Ziemons, *J. Pharm. Biomed. Anal.* **2018**, *147*, 458.

[2] J. Kiefer, *Am. Pharmaceut. Rev.* **2020**. https://www.americanpharmaceuticalreview.com/Featured-Articles/563939-Surface-Enhanced-Raman-Spectroscopy-for-Pharmaceutical-Analysis/ Accessed 18 November 2020

[3] M. T. Alula, Z. T. Mengesha, E. Mwenesongole, *Vib. Spectrosc.* **2018**, *98*, 50.

[4] E. Le Ru, P. Etchegoin, in *Principles of surface-enhanced Raman spectroscopy and related plasmonic effects*, (Eds: E. Le Ru, P. Etchegoin), Elsevier, Amsterdam **2009** 1.

[5] A. Balcytis, Y. Nishijima, S. Krishnamoorthy, A. Kuchmizhak, P. R. Stoddart, R. Petruskevicius, S. Juodkazis, *Adv. Optical Mater.* **2018**, *6*, 1800292.

Published in : Journal of Raman Spectroscopy (2022), vol. 53, n°1, pp. 20–32
DOI: 10.1002/jrs.6249
Status : Postprint (Author's version)

[6] R. Deidda, P.-Y. Sacré, M. Clavaud, L. Coïc, H. Avohou, P. Hubert, E. Ziemons, TrAC, *Trends Anal. Chem.* **2019**, *114*, 251.
[7] C. De Bleye, E. Dumont, C. Hubert, P. Y. Sacré, L. Netchacovitch, P.-F. Chavez, P. Hubert, E. Ziemons, *Anal. Chim. Acta* **2015**, *888*, 118.
[8] M. Fan, G. F. S. Andrade, A. G. Brolo, *Anal. Chim. Acta* **2020**, *1097*, 1.
[9] P. A. Mosier-Boss, *Nanomaterials* **2017**, *7*, 142.
[10] P. C. Lee, D. Meisel, *J. Phys. Chem.* **1982**, *86*(17), 3391.
[11] Y. Wang, E. Wang, Nanoparticle SERS Substrates, in *Surface Enhanced Raman Spectroscopy*, (Ed: S. Schlücker), Wiley-VCH, Weinheim **2011** 39.
[12] M. J. Vesga, D. McKechnie, S. Laing, H. Kearns, K. Faulds, K. Johnston, J. Sefcik, *Colloid Surf. A-Physicochem. Eng. Asp* **2021**, *621*, 126523.
[13] L. Yao, O. Jipint Lv, P. Dai, L. Zhu, *Microchem. J.* **2021**, *166*, 106221.
[14] J. He, H. Li, L. Zhang, X. Zhi, X. Li, X. Wang, Z. Feng, G. Shen, X. Ding, *Food Chem.* **2021**, *339*, 128085.
[15] E. Dumont, C. De Bleye, M. Haouchine, L. Coïc, P.-Y. Sacré, P. Hubert, E. Ziemons, *Spectrochim. Acta a* **2020**, *233*, 118180.
[16] E. C. Le Ru, P. G. Etchegoin, Metallic colloids and other SERS substrates, in *Principles of Surface-Enhanced Raman Spectroscopy and Related Plasmonic Effects*, (Eds: E. C. Le Ru, P. G. Etchegoin), Elsevier, Amsterdam **2009** 367.
[17] W. Xi, B. K. Shrestha, A. J. Haes, *Anal. Chem.* **2018**, *90*, 128.
[18] International Council for Harmonization of Technical Requirements for Pharmaceuticals for Human Use (ICH), ICH Q8 (R2) Pharmaceutical development, **2009**.
[19] S. Orlandini, S. Pinzauti, S. Furlanetto, *Anal. Bioanal. Chem.* **2013**, *405*, 443.
[20] P. Borman, M. Chatfield, P. Nethercote, D. Thompson, K. Truman, *Pharm. Technol.* **2007**, *31*, 142.
[21] E. Rozet, P. Lebrun, B. Debrus, B. Boulanger, P. Hubert, *Trends Analyt. Chem.* **2013**, *42*, 157.
[22] R. Deidda, S. Orlandini, P. Hubert, C. Hubert, *J. Pharm. Biomed. Anal.* **2018**, *161*, 110.
[23] F. G. Vogt, A. S. Kord, *J. Pharm. Sci.* **2011**, *100*, 797.
[24] P. K. Sahu, N. R. Ramisetti, T. Cecchi, S. Swain, C. S. Patro, J. Panda, *J. Pharm. Biomed. Anal.* **2018**, *147*, 590.
[25] P. Lebrun, B. Boulanger, B. Debrus, P. Lambert, P. Hubert, *J. Biopharm. Stat.* **2013**, *23*, 1330.
[26] R. H. Myers, D. C. Montgomery, C. M. Anderson-Cook, *Response Surface Methodology: Process and Product Optimization Using Designed Experiments*, John Wiley & Sons Inc., New Jersey, USA **2016**.
[27] J. Almeida, M. Bezerra, D. Markl, A. Berghaus, P. Borman, W. Schlindwein, *Pharmaceutics* **2020**, *12*, 150.
[28] H. Fisk, C. Westley, N. J. Turner, R. Goodacre, *J. Raman Spectrosc.* **2016**, *47*, 59.
[29] C. Levene, E. Correa, E. W. Blanch, R. Goodacre, *Anal. Chem.* **2012**, *84*, 7899.
[30] R. M. Jarvis, W. Rowe, N. R. Yaffe, R. O'Connor, J. D. Knowles, E. W. Blanch, R. Goodacre, *Anal Bioanal, Chel.* **2010**, *397*, 1893.
[31] P. Goos, J. Bradley, *Optimal Design of Experiments: A Case Study Approach*, John Wiley & Sons, Chichester, United Kingdom **2011**.
[32] J. J. Peterson, K. Lief, *Stat. Biopharm. Res.* **2010**, *2*, 249.
[33] E. Del Castillo, *Process Optimization: A Statistical Approach*, Springer Science & Business Media, New York, USA **2007**.
[34] R Core Team, R: A Language and Environment for Statistical Computing, R Foundation for Statistical Computing, Vienna, Austria, https://www.r-project.org/ (Accessed 3 June 2021).
[35] W. Wei, Q. Huang, *Spectrochim. Acta a Mol. Biomol. Spectrosc.* **2018**, *193*, 8.
[36] W. Tang, Y. An, K. H. Row, *Chem. Eng. J.* **2020**, *402*, 126194.
[37] Q. Sun, L. Zhang, L. Huang, R. Cai, D. Pan, H. Zeng, *Nanotechnology* **2020**, *31*, 305302.
[38] A. Tripathi, E. D. Emmons, N. D. Kline, S. D. Christesen, A. W. Fountain, J. A. Guichereau, *J. Physic. Chem.* **2018**, *122*, 10205.
[39] K. B. Bhavitha, A. K. Nair, S. Perumbilavil, S. Joseph, M. S. Kala, A. Saha, R. A. Narayanan, N. Hameed, S. Thomas, O. S. Oluwafemi, N. Kalarikkal, *Opt. Mater.* **2017**, *73*, 695.
[40] D. Zhang, P. Liang, Z. Yu, J. Huang, D. Ni, H. Shu, Q. Dong, *Sensors and Actuators B* **2018**, *256*, 721.